PROCEEDINGS OF SPIE

SPIEDigitalLibrary.org/conference-proceedings-of-spie

Quadratic neural networks for CT metal artifact reduction

Fenglei Fan, Hongming Shan, Lars Gjesteby, Ge Wang

Fenglei Fan, Hongming Shan, Lars Gjesteby, Ge Wang, "Quadratic neural networks for CT metal artifact reduction," Proc. SPIE 11113, Developments in X-Ray Tomography XII, 111130W (11 September 2019); doi: 10.1117/12.2530363

SPIE.

Event: SPIE Optical Engineering + Applications, 2019, San Diego, California, United States

Quadratic Neural Networks for CT Metal Artifact Reduction

Fenglei Fan, Hongming Shan, Lars Gjesteby, Ge Wang*
Biomedical Imaging Center, Department of Biomedical Engineering, Rensselaer Polytechnic Institute, Troy, New York, USA, 12180

ABSTRACT

Recently, deep learning has become the mainstream method in multiple fields of artificial intelligence / machine learning (AI/ML) applications, including medical imaging. Encouraged by the neural diversity in the human body, our group proposed to replace the inner product in the current artificial neuron with a quadratic operation on inputs (called quadratic neuron) for deep learning. Since the representation capability at the cellular level is enhanced by the quadratic neuron, we are motivated to build network architectures and evaluate the potential of quadratic neurons towards "quadratic deep learning". Along this direction, our previous theoretical studies have shown advantages of quadratic neurons and quadratic networks in terms of efficiency and representation. In this paper, we prototype a quadratic residual neural network (Q-ResNet) by incorporating quadratic neurons into a convolutional residual structure, and then deploy it for CT metal artifact reduction. Also, we report our experiments on a simulated dataset to show that Q-ResNet performs better than the classic NMAR algorithm.

Keywords: Deep learning, quadratic neurons, quadratic residual networks, metal artifact reduction (MAR).

1. INTRODUCTION

Over the recent years, deep learning has been transforming many fields including medical imaging [1-5]. The spectrum of deep learning research spans from theoretical studies to architectural innovations, i. e. VGG [6], Res-Net [7], GAN [8], AutoML [9] etc. These advancing network structures are critical for superior performance of deep learning systems, having achieved successes in various supervised and unsupervised tasks.

Encouraged by the success of neural diversity observed in the human body, our group proposed to replace the inner product in the current artificial neuron with a quadratic operation on inputs (called quadratic neuron) for deep learning [10-12]. At the cellular level, the representation ability of the quadratic neuron is enhanced; for instance, even an individual quadratic neuron can realize any logic/fuzzy logic operation including XOR, which is impossible for the conventional neuron. Furthermore, we theoretically revealed the advantages of quadratic networks over conventional networks in terms of efficiency and representation [13]. Naturally, we are curious if quadratic networks can produce state-of-the-art results in solving real-world problems, thereby translating quadratic deep learning tools into suitable machine learning applications.

Metal artifact reduction (MAR) is a long-standing problem in the CT field, which greatly impedes diagnosis and therapy based on CT images. Although the improvements of varying degree were realized in the past decades [14], there are remaining artifacts in important applications for which even the state-of-the art MAR algorithm cannot provide satisfactory results. Current MAR techniques can be classified into four categorizations [14]: acquisition improvements, physics-based pre-processing, iterative reconstruction, and post-processing [21,22]. However, due to the metal-induced information loss, classic post-processing methods can only claim a limited victory in most challenging tasks.

As the first step to forge a pragmatic quadratic network for metal artifact reduction, here we propose a quadratic residual network, which solely constitutes quadratic neurons at each layer, optimizing the pathway of how features are extracted. Heuristically speaking, the physical world is described by 2nd order equations, and the information world abounds with quadratic features. Therefore, a deep quadratic residual network seems proper, and ought to be effective in extracting useful features from images. Our further hypothesis specific to the MAR problem is that the quadratic neuron is naturally focused on quadratic features and can be "immune" to the annoying streaks which has linear character, therefore facilitating the recovery of the hidden structure from streaks.

*corresponding author, please contact wangg6@rpi.edu.

Developments in X-Ray Tomography XII, edited by Bert Müller, Ge Wang, Proc. of SPIE Vol. 11113, 111130W · © 2019 SPIE
CCC code: 0277-786X/19/$21 · doi: 10.1117/12.2530363

To put our study in perspective, we would like to acknowledge that there are results in the literature that suggested high-order or nonlinear representation ideas as well, either implicitly or explicitly. For instance, high-order neurons have spun up in the early stage of artificial intelligence. However, they were never really linked to deep networks because of trainability issues, particularly difficulties in tackling with the combinatorial explosion. Nevertheless, our quadratic network accomplishes a high-order nonlinear representation through many layers in an efficient way which circumvents the parameter explosion, and our deep quadratic network can be practically trained using modern optimization methods on a high-performance computing platform, enabling a large-scale optimization for real-world problems. Livni et al. [15] and Krotov et al. [16] altered the activation function of neurons to a quadratic form: $\sigma(z) = z^2$, but such a kind of nonlinearity is not truly nonlinearity because the decision boundary is still linear for those neurons. Tsapanos et al. [17] proposed a parabolic neuron, which is actually a special case of a quadratic neuron. Lin et al. [18] proposed the so-called network in network (NIN) by moving the micro-networks across the input images so that complex nonlinear features can be directly collected. Wang et al. [19] studied second-order operations for deep learning using a cross product of two network branches, but their method only processes features post-hoc, which are extracted by two conventional networks.

2. METHODOLOGY

Before we describe our quadratic residual network, let us first introduce basics regarding quadratic neurons and "quadratic convolution", which is the generalization of the convolutional operation for deep learning.

Quadratic Neurons: A quadratic neuron is an upgraded version of a traditional neuron based on the inner product. Mathematically, the quadratic neuron first aggregates the n-dimension input $\boldsymbol{x}$ in Eq. (1) (other forms of quadratic aggregation are possible but beyond the scope of this manuscript):

$$\begin{aligned} h(\boldsymbol{x}) &= (\sum_{i=1}^{n} w_{ir} x_i + b_r)(\sum_{i=1}^{n} w_{ig} x_i + b_g) + \sum_{i=1}^{n} w_{ib} x_i^2 + c \\ &= (\boldsymbol{w_r x^T} + b_r)\left(\boldsymbol{w_g x^T} + b_g\right) + \boldsymbol{w_b}(\boldsymbol{x^2})^T + c. \end{aligned} \tag{1}$$

Next, the function value $h(\boldsymbol{x})$ will be passed into a nonlinear activation $\sigma(\cdot)$ such as ReLU to define the output:

$$g(\boldsymbol{x}) = \sigma\big(h(\boldsymbol{x})\big), \tag{2}$$

where $g(\boldsymbol{x})$ is the definition of our quadratic neuron. It is underlined that our definition of a quadratic neuron only uses $3n$ parameters, which is much sparser than the general quadratic representation requiring $\frac{n(n+1)}{2}$ parameters.

Quadratic "Convolution" (Q-Conv): The convolutional neural network (CNN) is the most significant architecture for deep learning. In the circumstance of quadratic networks, each feature map is obtained by sliding a quadratic neuron over an input field in a similar manner as a micro network does in the context of NIN. Strictly speaking, such a quadratic operation is not a convolution, but it can be regarded as a nonlinear convolution heuristically.

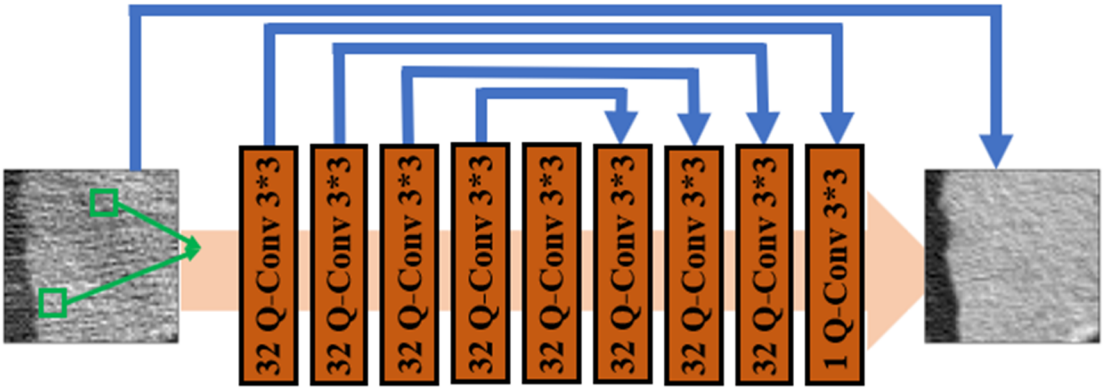

Figure 1. Architecture of the quadratic residual network (Q-ResNet).

Quadratic Residual Network (Q-ResNet): The architecture of our quadratic residual network is shown in Figure 1. In total, the quadratic residual network has 10 fully convolutional layers with 32 3*3 quadratic convolutional kernels in each layer. Zero padding is used to keep the size of images intact. The optimization model minimizing the mean square error can be expressed as follows:

$$\underset{\boldsymbol{W}}{\operatorname{argmin}} \ \|Y - \boldsymbol{H}(\boldsymbol{W}, \boldsymbol{X})\|_2^2 \tag{3}$$

where $\boldsymbol{X}$ is the input image, Y is the ground-truth image and H is the function represented by Q-ResNet.

3. RESULTS

We evaluated our Q-ResNet for metal artifact reduction with a simulated clinical dataset. Two sets of voxelized phantoms were produced from the volumetric data in the pelvic and spinal region. Then Titanium was inserted in the femoral head regions and vertebrae to simulate a hip prosthesis and spinal fixation rods respectively. We used an industrial CT simulation software *CatSim* [23] to scan both sets of phantoms to generate the artifact-free projections and metal-disturbed projections. *CatSim* models the parameters of a real physical system with the authentic effects such as scatter, beam hardening, quantum noise and electronic noise. The reconstructed images of the metal-inserted phantoms are of size 512*512 containing severe artifacts. Instead of directly recovering images from raw degraded images, we first apply a custom implementation of the classic NMAR [20] algorithm to perform initial correction on the raw images. NMAR is based on sinogram interpolation hence the images after NMAR processing contain more information than the corresponding raw images. We feed the NMAR images into our Q-ResNet, while the images without metal inserted serve as ground truth. The phantom pairs with a total of 50 images were scanned at 1mm-thickness. Forty-two of these images were for training, and eight were reserved for evaluation. Specifically, 38,000 image patches were extracted from training slices and 5965 image patches were extracted for evaluation. For the training, we used the batch training with batch size of 50 in each step and we have 60 epochs wherein each epoch exhausted all the samples in training dataset. The optimization method is Adam. The learning rate is $1e^{-4}$ in the first 30 epochs and halved in the second 30 epochs.

Training: We plotted the dynamics of training loss and validation loss with respect to epochs. As Figure 2 shown, the training loss and validation loss descends concordantly, indicating no overfitting is taking place. Even though the quadratic neuron utilizes more parameters in the cellular level, our Q-ResNet here avoids overfitting because the more efficient structure is used, resulting that the overall model complexity is low.

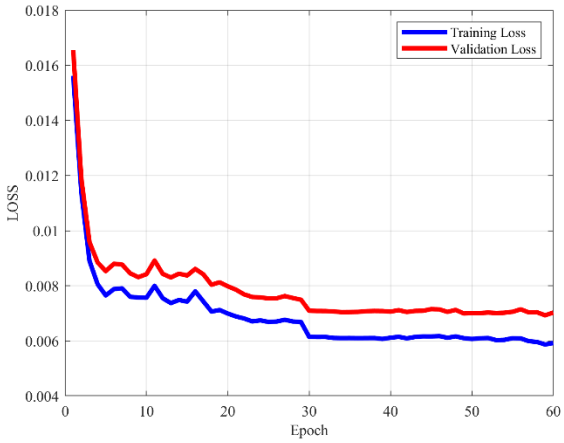

Figure 2. The training loss and evaluation loss descends concordantly, which means the learning of Q-ResNet is well-fitted.

Imaging Performance: We further applied our trained Q-ResNet to two full-size images withheld from training and validation set. The results are shown in Figure 3 and Figure 5. In Figure 3, the initial uncorrected reconstruction performs poorly, a dark band in the middle of the images severely degrades the image quality. NMAR effectively provides higher-quality reconstruction. However, there still remained non-negligible streaks in NMAR images. In contrast, it is clear seen that the Q-ResNet further suppresses the streak artifacts existing NMAR image. In Figure 5, the white streaks perpetuate in the uncorrected image and NMAR image, but Q-ResNet clearly cancelled the streaks,

though the image becomes slightly smoother. In the zoomed ROIs of Figure 3 and Figure 5 (Figure 4 and Figure 6, respectively), the Q-ResNet images show less significant streaks and clearer anatomy.

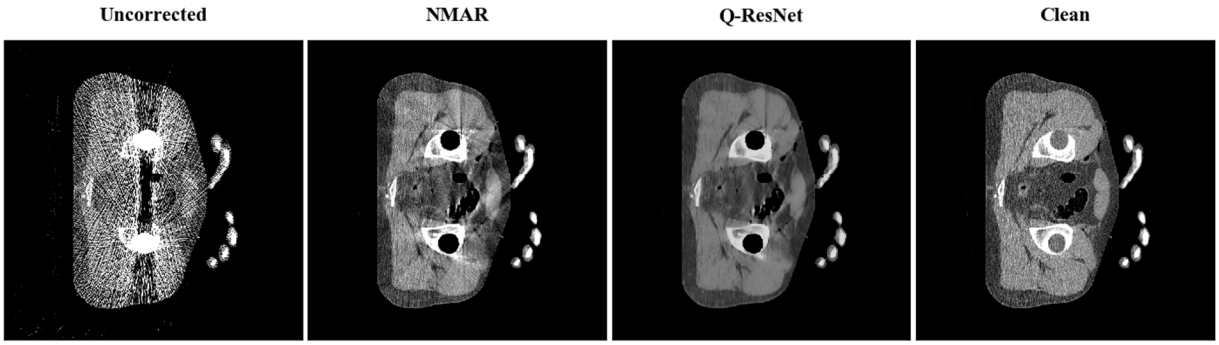

Figure 3. Hip prostheses case. Left to right: Initial uncorrected reconstruction; NMAR-corrected images; Reconstruction using Q-ResNet; Artifact-free truth. Q-ResNet reconstruction clearly eliminates more streak artifact than the baseline NMAR.

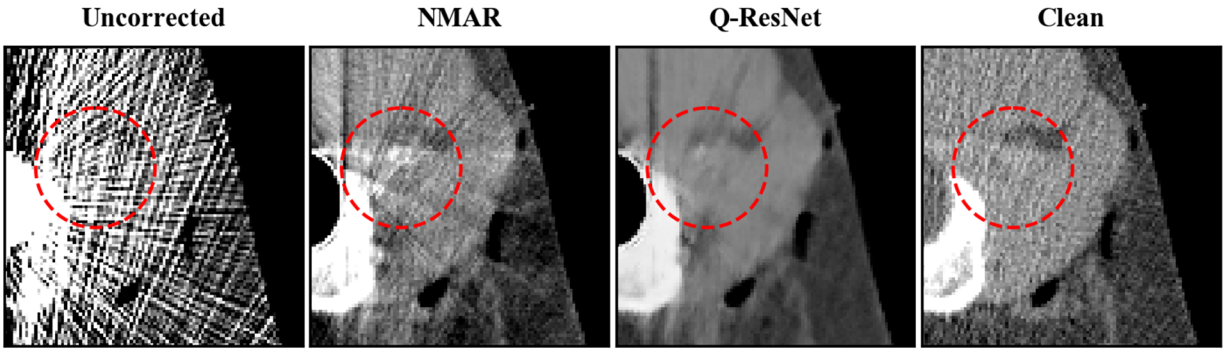

Figure 4. Zoomed ROI of Figure 3. Less artifacts are present in the Q-ResNet reconstruction compared to the NMAR image.

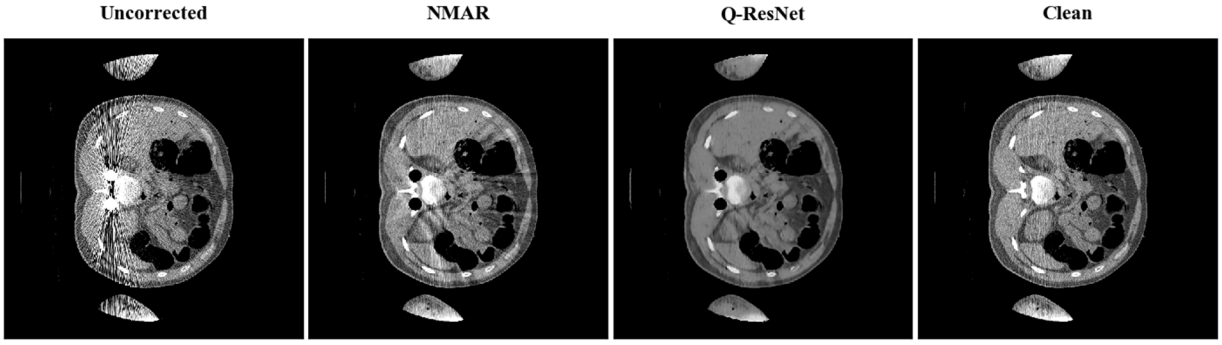

Figure 5. Spinal fixation rods case. From left to right: Initial uncorrected reconstruction; NMAR-corrected images; Reconstruction using Q-ResNet; Artifact-free truth. Q-ResNet reconstruction clearly suppresses the streak artifacts existing in the NMAR and uncorrected images.

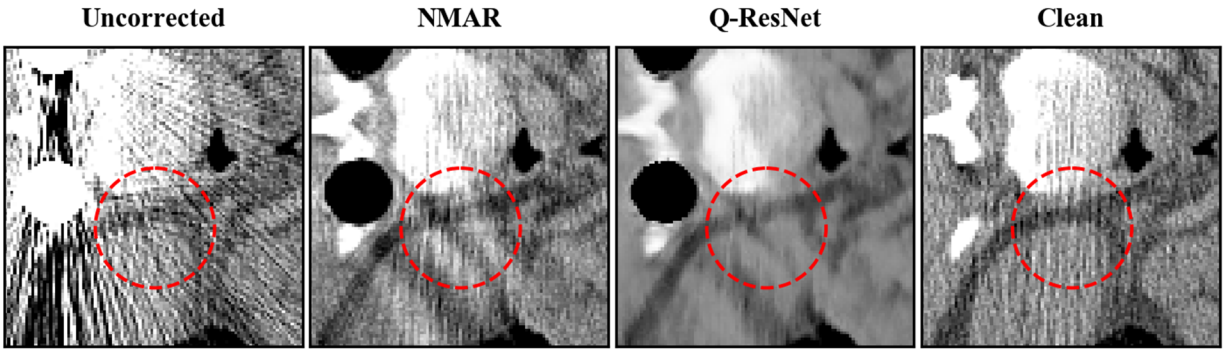

Figure 6. Zoomed ROI of Figure 5. The anatomy is noticeably flatter in the Q-ResNet reconstruction than NMAR image.

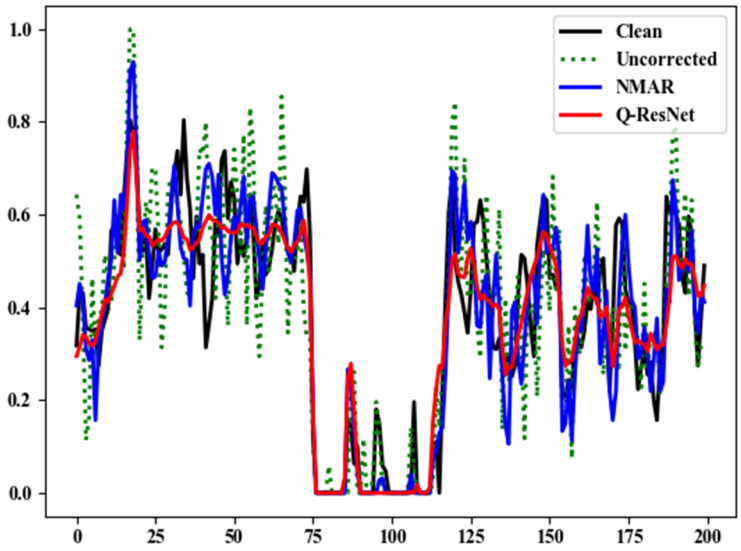

Figure 7. Profiling of center of four sub-images in Figure 5. It is seen that the Q-ResNet model drives down the streak artifacts.

Further we look at the profiling of center of four sub-images in Figure 5. It is observed that Q-ResNet albeit achieved smoother curve but it successfully alleviates streak artifacts.

We also employed the common quantitative measures peak signal noise ratio (PSNR), structural similarity measure (SSIM), and rooted mean square error (RMSE) to compare the recovery performance of Q-ResNet and NMAR on Figure 3 and Figure 5. The results are summarized in TABLE I. It is underscored that both NMAR and Q-ResNet algorithm improve the image quality from uncorrected images in terms of PSNR, SSIM, and RMSE. However, Q-ResNet produces images of even better quality. The gain is particularly large in Figure 4.

TABLE I: QUANTITATIVE COMPARISON OF THE RECOVERY PERFORMANCE USING DIFFERENT ALGORITHMS FOR METAL ARTIFACTS

	Figure 4			Figure 5		
	PSNR	SSIM	RMSE	PSNR	SSIM	RMSE
Uncorrected	13.41	0.6795	0.2134	18.98	0.8117	0.1124
NMAR	20.47	0.7924	0.0947	23.20	0.8619	0.0691
Q-ResNet	**21.78**	**0.8053**	**0.0813**	**23.93**	**0.8626**	**0.0635**

4. CONCLUSION

In conclusion, we have reported the architecture and utility of our Q-ResNet for metal artifact reduction problem. We are motivated to promote the use of quadratic neuron based deep neural networks. Our results suggest that quadratic deep learning has a potential in machine learning. Future studies along this track are in progress, in hope that quadratic neuron deep learning will solve more real-world problems.

REFERENCE

[1] Y. LeCun, Y. Bengio, and G. Hinton, "Deep learning," Nature, **521**(7553), 436, 2015.

[2] G. Wang, "A perspective on deep imaging," arXiv preprint arXiv:1609.04375, 2016.

[3] Chen. H., Zhang, Y., Zhang, W., Liao, P., Li, K., Zhou, J., & Wang, G. (2017). Low-dose CT via convolutional neural network. Biomedical optics express, 8(2), 679-694.

[4] Shan, H., Zhang, Y., Yang, Q., Kruger, U., Kalra, M. K., Sun, L., ... & Wang, G. (2018). 3-D convolutional encoder-decoder network for low-dose CT via transfer learning from a 2-D trained network. IEEE transactions on medical imaging, 37(6), 1522-1534.

[5] Lyu, Q., You, C., Shan, H., & Wang, G. (2018). Super-resolution MRI through Deep Learning. arXiv preprint arXiv:1810.06776.

[6] K. Simonyan, A. Zisserman, "Very deep convolutional networks for large-scale image recognition," In ICLR, 2015.

[7] He, K., Zhang, X., Ren, S., & Sun, J. (2016). Deep residual learning for image recognition. In Proceedings of the IEEE conference on computer vision and pattern recognition (pp. 770-778).

[8] Goodfellow, I., Pouget-Abadie, J., Mirza, M., Xu, B., Warde-Farley, D., Ozair, S., ... & Bengio, Y. (2014). Generative adversarial nets. In Advances in neural information processing systems (pp. 2672-2680).

[9] Zoph, B., & Le, Q. V. (2016). Neural architecture search with reinforcement learning. arXiv preprint arXiv:1611.01578.

[10] Fan, F., Cong, W., & Wang, G. (2018). A new type of neurons for machine learning. International journal for numerical methods in biomedical engineering, 34(2), e2920.

[11] Fan, F., Cong, W., & Wang, G. (2018). Generalized backpropagation algorithm for training second‐order neural networks. International journal for numerical methods in biomedical engineering, 34(5), e2956.

[12] Fan, F., & Wang, G. (2018). Universal Approximation with Quadratic Deep Networks. arXiv preprint arXiv:1808.00098.

[13] Fan, F., & Wang, G. (2018). Fuzzy Logic Interpretation of Artificial Neural Networks. arXiv preprint arXiv:1807.03215

[14] Gjesteby, L., De Man, B., Jin, Y., Paganetti, H., Verburg, J., Giantsoudi, D., & Wang, G. (2016). Metal artifact reduction in CT: where are we after four decades?. IEEE Access, 4, 5826-5849.

[15] Livni, R., Shalev-Shwartz, S., & Shamir, O. (2014). On the computational efficiency of training neural networks. In Advances in neural information processing systems (pp. 855-863).

[16] D. Krotov and J. Hopfield, "Dense associative memory is robust to adversarial inputs," Neural computation, 30(12), 3151-3167, 2018

[17] N. Tsapanos, A. Tefas, N. Nikolaidis and I. Pitas, "Neurons With Paraboloid Decision Boundaries for Improved Neural Network Classification Performance," IEEE Trans. Neural. Netw. Learn. Syst., vol. 99, pp.1-11.

[18] Lin, M., Chen, Q., & Yan, S. (2013). Network in network. arXiv preprint arXiv:1312.4400

[19] Wang, Y., Xie, L., Liu, C., Qiao, S., Zhang, Y., Zhang, W., ... & Yuille, A. (2017). Sort: Second-order response transform for visual recognition. In Proceedings of the IEEE International Conference on Computer Vision (pp. 1359-1368).

[20] Meyer, E., Raupach, R., Lell, M., Schmidt, B., & Kachelrieß, M. (2010). Normalized metal artifact reduction (NMAR) in computed tomography. Medical physics, 37(10), 5482-5493.

[21] Gjesteby L, Shan H, Yang Q, Xi Y, Claus B, Jin Y, De Man B, Wang G. Deep Neural Network for CT Metal Artifact Reduction with a Perceptual Loss Function. InIn Proceedings of The Fifth International Conference on Image Formation in X-ray Computed Tomography 2018

[22] Gjesteby L, Yang Q, Xi Y, Shan H, Claus B, Jin Y, De Man B, Wang G. Deep learning methods for CT image-domain metal artifact reduction. In Developments in X-Ray Tomography XI 2017 Sep 25 (Vol. 10391, p. 103910W)

[23] De Man B., Basu S., Chandra N., Dunham B., Edic P., Iatrou M., McOlash S., Sainath P., Shaughnessy C., Tower B., et al., "Catsim: a new computer assisted tomography simulation environment," in Medical Imaging 2007: Physics of Medical Imaging, vol. 6510, p. 65102G, International Society for Optics and Photonics, 2007.